BULLETIN OF THE POLISH ACADEMY OF SCIENCES
TECHNICAL SCIENCES, Vol. 60, No. 2, 2012
DOI: 10.2478/v10175-012-0036-3

An investigation of nonlinear tangential contact behaviour of a spherical particle under varying loading

D. ZABULIONIS[1]*, R. KAČIANAUSKAS[1], D. MARKAUSKAS[1], and J. ROJEK[2]

[1] Laboratory of Numerical Modelling, Vilnius Gediminas Technical University, 11 Saulėtekio Ave., 10223 Vilnius, Lithuania
[2] Insitute of Fundamental Technological Research, Polish Academy of Sciences, 5B Pawinskiego St., 02-106 Warsaw, Poland

Abstract. An analytical and numerical study of the tangential contact of a spherical particle under varying combined normal-tangential loading is presented. The normal and tangential contact is described by the Hertz and regularized Coulomb laws. This study is focused on the analysis of the tangential displacement of the particle's contact point under variable normal force and reevaluation of the procedures for calculation of the tangential force. The incremental displacement-driven and force-driven constitutive relationships are developed. The importance of an adequate numerical treatment of the tangential component of the contact force is shown for the slide mode, and the recommendations for its evaluation are proposed. The performance of the algorithm is demonstrated by solving the problem of the oblique impact of the spherical particle on the wall. The suggested methodology allows us to analyse the elastic and sliding effects of the tangential interaction more precisely than existing methodologies. Besides, the issue of the direction of the tangential force, when the Coulomb limit is reached, was reconsidered in one-dimensional case by taking three versions of the unit direction vector, which are based on the tangential elastic displacement, tangential stick force, and tangential relative velocity of the contact point of the particle.

Key words: discrete element method, tangential elastic-frictional contact, incrementally linear constitutive relationship, stick-sliding switch.

List of symbols

$\|\| \bullet \|\|$	–	norm or length of the vector,
$\mathbf{d}_C$	–	vector connecting contact point and particle mass centre,
E	–	particle's and wall's elastic modulus,
$\mathbf{F}$	–	force acting on a particle centre,
$\mathbf{F}_n$, $\mathbf{F}_n^*$	–	normal and normalized normal forces acting at the particle contact point,
$\mathbf{F}_t$	–	tangential force acting at the particle contact point,
$\mathbf{F}_{t,sl}$	–	sliding frictional force acting at the particle contact point,
$\mathbf{F}_{t,st}$	–	stick frictional force acting at the particle contact point,
G	–	particle's and wall's shear modulus,
h	–	contacting bodies overlap or their relative normal displacement,
I	–	second moment of inertia of the particle,
k_n, k_n^*	–	normal and normalized normal interaction stiffnesses,
k_t, k_t^*	–	tangential and normalized tangential interaction stiffnesses,
$\mathbf{M}$	–	particle moment acting on a particle centre,
M	–	particle mass,
$\mathbf{n}$	–	unit vector of the normal interaction,
$proj_{\mathbf{a}}\mathbf{b}$	–	projection of the vector $\mathbf{b}$ onto vector $\mathbf{a}$,
R	–	particle radius,
$\mathbf{s}$	–	contact point total displacement,
t and t^*	–	time and normalized time,
$\mathbf{t}$	–	unit vector of the tangential interaction,
$t_{c,0}$	–	beginning time of the contact,
$t_{c,dur}$	–	duration of the contact,
ν	–	particle's and wall's Poison's modulus,
$\mathbf{v}$	–	velocity vector of the particle's mass centre,
$\mathbf{v}_C$	–	relative velocity of the particle's contact point,
$\mathbf{v}_{C,n}$	–	normal component of the relative velocity of the particle's contact point,
$\mathbf{v}_{C,t}$	–	tangential component of the relative velocity of the particle's contact point,
$\mathbf{v}_n$	–	normal component of the particle's centre velocity,
$\mathbf{v}_t$	–	tangential component of the particle's centre velocity,
$\mathbf{x}$	–	displacement vector,
α	–	attack angle,
Δ	–	increment or difference,
$\boldsymbol{\delta}_{el}$	–	tangential elastic displacement,
$\boldsymbol{\delta}_{sl}$	–	contact point sliding displacement,
$\boldsymbol{\varepsilon}$	–	angular acceleration,
$\boldsymbol{\theta}$	–	angular displacement,
μ	–	coefficient of the sliding friction,
η	–	optional coefficient varying between 0 and 1,
$\boldsymbol{\omega}$	–	angular velocity vector.

*e-mail: Darius.Zabulionis@vgtu.lt

1. Introduction

Computer simulation is a fundamental research tool for getting a thorough understanding of complex material structures and it provides a feasible alternative to physical experiments. The Discrete Element Method (DEM) introduced by Cundall and Strack [1] has been widely recognised as the most suitable numerical technique for simulating behaviour of granular materials on both microscopic and macroscopic scales.

The DEM is a discrete, particle-oriented method tracking the motion of each individual particle and its interactions with neighbouring particles and other objects over time. The rigid-body motion of a particle is described in the framework of classical mechanics. Thereby, the required dynamic equilibrium of all the forces and torques at each particle is assumed to be satisfied during the considered period of time adopting an incremental time integration procedure.

Analysis of the contact behaviour of the interacting particles is the most important aspect in the DEM. The application of the DEM in simulation of the granular materials has enormously increased in the past two decades. Various linear and nonlinear contact models of different complexity were elaborated. It is worth mentioning, that the vectors at the particle's contact point are usually separated into the normal and tangential components. In this work, a special attention will be given to evaluation of the tangential component.

In most studies, the contact of particles is treated assuming the linear Kelvin model in the normal direction, suggested by Cundall and Strack [1], and the Kelvin model with a slider in the tangential direction. Nonlinear models of the normal and tangential contact are based on the Hertz, Mindlin and Deresiewicz theories [2, 3].

Comprehensive reviews of theoretical contact models were presented by Džiugys and Peters [4], Zhou [5], Kruggel-Emden [6] and Thornton [7]. Zhang [8] and Kruggel-Emden [10] reviewed tangential models that account for interfacial friction, elastic and plastic deformations. Kruggel-Emden [11] presented the theoretical solution of the elastic contact between two homogeneous spheres in the normal direction, as well.

Let us focus on the tangential elastic-frictional contact. In the present article, the regularized Coulomb law is characterised by the incrementally linear force-displacement relationship in the elastic range. The tangential force is bounded by the Coulomb limit, which is expressed in terms of the friction coefficient μ and normal force $\mathbf{F}_n$. In the DEM, the models of non-cohesive dry elastic normal and tangential contact are mostly treated independently. Incrementally linear models reveal a nonlinear dependence of the tangential force on the tangential displacement. Important contributions for modelling of the nonlinear contact were made by Walton and Braun [12], Tsuji et al. [13], Di Renzo and Di Maio [14], and Brilliantov [16]. These authors considered a hysteric behaviour of the tangential contact. In contrast, a combination of the full integral forms of the Hertz and Mindlin-Deresiewicz formulations provides a non-linear model, which is able to trace the entire loading history of contact. Due to complexity of the contact history applications of the Hertz and Mindlin-Deresiewicz models are still limited. A discussion on loading-unloading-reloading modes of the particle and computational details was continued by Zhang and Vu-Quoc [8, 9], Di Renzo [14], Kruggel-Emden [10] and Thornton [7].

The behaviour of a particle in the tangential direction as well as the conformity with the theoretical methods and experimental results is still an open question in DEM. The behaviour of the sliding and post-sliding hysteretic contact has not been clearly explained yet.

Thornton [7] reconsidered typical models of the tangential interactions of DEM without damping. He [7] and Kruggel-Emden [10] showed that a non-incremental scheme of the tangential force has disadvantages in comparison with an incremental scheme. Thornton [7] also pointed out that the linear approach for recalculation of the elastic displacement of the contact point is incompatible with the incremental scheme of the tangential force when the Coulomb limit is reached.

There are still some problems with modelling of the tangential interaction of the particle. Firstly, it concerns the selection of the mentioned above interaction laws: linear, incrementally linear or nonlinear. Secondly, the evaluation of the transition points from stick to slide and vice versa or the change of the vectors sign is numerically sensitive. Comments on the issue are skipped, however, in the majority of publications.

The first goal of our article is the theoretical analysis and numerical implementation of the recalculation of the elastic displacement of the tangential contact when the Coulomb limit is reached. Our analysis showed that the linear approach for recalculation of the tangential displacement is proper only when the tangential stiffness of the particle interaction is constant during the contact. Otherwise the tangential elastic displacement may have discontinuity at the stick-sliding point.

The second goal of our article is to evaluate the unit direction vector $\mathbf{t}$. The analysis of the literature shows that there are three versions of the unit tangent vector $\mathbf{t}$ of the tangential force $\mathbf{F}_t$ when Coulomb limit is reached: $\mathbf{t} = -\mathbf{v}_{C,t}/||\mathbf{v}_{C,t}||$ [17–19], $\mathbf{t} = \mathbf{F}_{t,st}/||\mathbf{F}_{t,st}||$ [20, 21] and $\mathbf{t} = -\boldsymbol{\delta}_{el}/||\boldsymbol{\delta}_{el}||$ [14], where $\mathbf{v}_{C,t}$ is the tangent component of the relative velocity at the contact point, and the symbol $||\ \ ||$ denotes Euclidean norm. Our calculations showed that these three vectors are not equivalent during the contact period starting at the point when the relative tangential velocity of the contact point equals zero and the Coulomb limit is reached.

The paper is organised as follows. The formulation of the DEM and the approaches to modelling the tangential contact are described in Sec. 2. The incremental, history dependent constitutive relationships are developed and described in Sec. 3. The numerical solution of the oblique impact of a spherical particle on an elastic plane and performance of the developed approach are given in Sec. 4. The sensitivity of the results on the unit tangent vectors is demonstrated and discussed in Sec. 5, while conclusions are formulated in Sec. 6. The used integration algorithm is presented in the Appendix.

2. DEM methodology

Investigation of the tangential contact is performed in the framework of the Discrete Element Method. The DEM is a numerical method investigating a particulate material as a system of a finite number of contacting particles. Each particle i is assumed to be characterized by the prescribed shape, in our case sphere with radius R_i, the material properties and the constitutive interaction laws. Physical properties of each elastic particle are constant and defined by the density ρ, modulus of elasticity E and Poisson's ratio ν.

A 3D motion of an arbitrary particle is characterized by the following vectors: the position vector $\mathbf{x}_i$ of the particle mass centre with respect to the fixed Cartesian frame $\mathbf{X}$, the translational velocity $\mathbf{v}_i = \dot{\mathbf{x}}_i = d\mathbf{x}_i/dt$ and the acceleration $\mathbf{a}_i = \dot{\mathbf{v}}_i = \ddot{\mathbf{x}}_i$, as well as the vectors of angular velocity $\boldsymbol{\omega}_i$ and angular acceleration $\boldsymbol{\varepsilon}_i = \dot{\boldsymbol{\omega}}_i$. In an arbitrary three-dimensional motion, the rotational position cannot be defined by any vector; therefore, the rotational velocity $\boldsymbol{\omega}_i$ cannot be integrated, cf. Argyris [22]. An angular orientation of the particle can be defined by the rotation matrix $\boldsymbol{\Lambda}_i$, which specifies the rotation between the fixed Cartesian frame $\mathbf{X}$ and the Cartesian frame $\mathbf{x'}_i$ embedded in the particle

$$\mathbf{X} = \boldsymbol{\Lambda}_i \mathbf{x'}_i. \tag{1}$$

Moving particles obey Newton's second law and their motion in time t is described by the following set of ordinary differential equations

$$m_i \ddot{\mathbf{x}}_i(t) = \mathbf{F}_i(t), \tag{2}$$

$$I_i \dot{\boldsymbol{\omega}}_i(t) = \mathbf{M}_i(t), \tag{3}$$

where m_i and I_i are mass and moment of the inertia of the i^{th} particle, respectively. The vectors $\mathbf{F}_i$ and $\mathbf{M}_i$ present the resultants of the external and interaction forces and torques, which act in the centres of the particles. Thereby, evaluation of the interaction forces will be conducted in the framework of the DEM considering independently contact of each pair of colliding objects (two particles or a particle and a wall).

Let us identify colliding objects in the following manner. Two interacting particles may be denoted by the subscripts i and j while the wall is denoted by the subscript w. Quantities related to the particle-particle interaction are denoted usually by the pair of subscripts *ij* or *ji*; hence, the quantities related to the particle-wall interaction may be denoted by the subscripts *iw* or *jw*, respectively. To unify notations given below for both particle-particle and particle-wall interactions, the subscripts i, j and w are replaced with the symbols α and β, where $\alpha, \beta \in \{i, j, w\}$. Consequently, the combination α, β is used to represent the subscripts *ij*, *ji*, *iw* or *jw*. Since the interaction is binary, it is evident that $\alpha \neq \beta$.

It should be noticed that all the interaction variables will be presented in terms of the normal and tangential components denoted hereafter by the subscripts n and t.

2.1. Interaction geometry and kinematics. The geometry of two interacting particles and most important variables are presented in Fig. 1. The vector $x_{\alpha\beta} = x_\alpha - x_\beta$, where $\alpha, \beta \in \{i, j\}$, connects the centres of the particles i and j, moreover, $\mathbf{x}_{\alpha\beta} = -\mathbf{x}_{\beta\alpha}$. It is generally agreed that the resultant of the interaction force between the particles i and j acts at the so-called contact point C. In the case of two equal spherical particles, the contact point C lies at the midpoint of the vector $\mathbf{x}_{\alpha\beta}$. In the case of the particle-wall contact, the contact point C lies on the line that is perpendicular to the wall and passes through the centre of the particle.

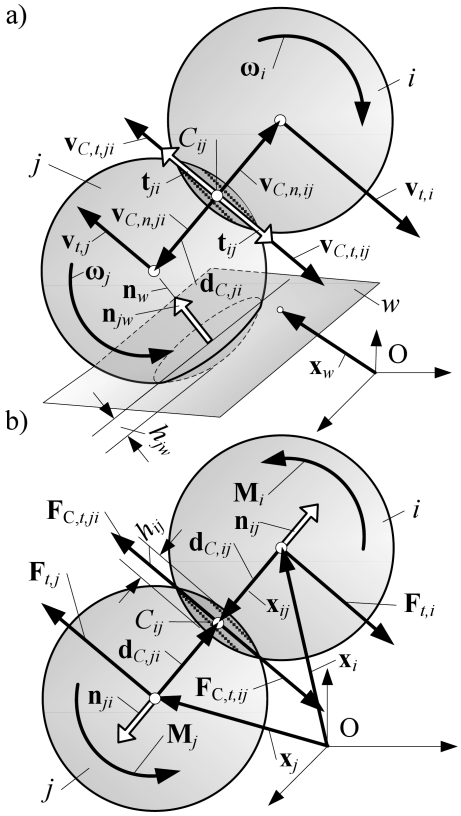

Fig. 1. The geometry of the interacting particles: a) vectors of the translational and angular velocities, b) vectors of the positions and forces

The normal direction of the contact is characterised by the unit vector $\mathbf{n}_{\alpha\beta}$

– for particle-particle interaction

$$\mathbf{n}_{\alpha\beta} = \mathbf{x}_{\alpha\beta}/\|\mathbf{x}_{\alpha\beta}\|, \quad \alpha, \beta \in \{i, j\}, \tag{4}$$

– for particle–wall interaction

$$\mathbf{n}_{\alpha w} = \mathbf{n}_w, \quad \alpha \in \{i, j\}. \tag{5}$$

The normal interaction of colliding objects is described by their overlap h termed in DEM as the normal displacement. For two colliding particles α and β the overlap h, $h \equiv h_{\alpha\beta}$, can be expressed from the interaction geometry (Fig. 1) as follows

$$h = R_\alpha + R_\beta - \|\mathbf{x}_{\alpha\beta}\|, \quad \alpha, \beta \in \{i, j\}, \tag{6}$$

where R_α and R_β are the particles' radii, while subscripts *ij* or $\alpha\beta$ will be omitted for the sake of simplicity.

For the particle-wall contact h, $h \equiv h_{\alpha w}$, is expressed as

$$h = R_\alpha - \mathbf{n}_w \bullet (\mathbf{x}_\alpha - \mathbf{x}_w), \quad \alpha \in \{i, j\}, \tag{7}$$

where the dot sign • stands for the scalar product, while $\mathbf{x}_w$ is the vector characterizing the plane location. This vector begins at the origin of the coordinate system, while its end belongs to the plane.

The position of the contact point with respect to the centre of the particle α is specified by the vector $\mathbf{d}_{C,\alpha\beta}$, $\alpha, \beta \in \{i, j, w\}$, (Fig. 1). It begins at the centre of the particle and ends at the contact point C

$$\mathbf{d}_{C,\alpha\beta} = -\left(R_\alpha - 1/2h\right)\mathbf{n}_{\alpha\beta}. \tag{8}$$

The relative translational velocity $\mathbf{v}_{C,\alpha\beta}$ of the contact point C of the particle α with respect to the contact point C of the particle β is expressed via the velocities of particles as follows

$$\mathbf{v}_{C,\alpha\beta} = \mathbf{v}_\alpha + \boldsymbol{\omega}_\alpha \times \mathbf{d}_{C,\alpha\beta} - \mathbf{v}_\beta - \boldsymbol{\omega}_\beta \times \mathbf{d}_{C,\beta\alpha}, \tag{9}$$

where $\mathbf{v}_\alpha$, $\mathbf{v}_\beta$, $\boldsymbol{\omega}_\alpha$ and $\boldsymbol{\omega}_\beta$ are translational and angular velocities of the respective particles' centres, the sign $\times$ denotes the cross product. For the particle-wall contact, the relative velocity $\mathbf{v}_{C,\alpha w}$, $\alpha \in \{i, j\}$ is also calculated according to (9), assuming that angular velocity of the wall $\boldsymbol{\omega}_w = \boldsymbol{\omega}_\beta = 0$.

The normal and tangential components of the relative velocity $\boldsymbol{v}_{C,\alpha\beta}$ of the contact points C are calculated by applying vector rules as follows

$$\mathbf{v}_{C,n,\alpha\beta} = \left(\mathbf{v}_{C,\alpha\beta} \bullet \mathbf{n}_{\alpha\beta}\right)\ \mathbf{n}_{\alpha\beta}, \tag{10}$$

$$\mathbf{v}_{C,t,\alpha\beta} = \mathbf{v}_{C,\alpha\beta} - \mathbf{v}_{C,n,\alpha\beta}. \tag{11}$$

2.2. Particle interaction models. Particle interaction models comprise relationships between the contact forces and displacements. The contact force between the particles α and β is presented by a composition of the normal and tangential components

$$\mathbf{F}_{\alpha\beta} = \mathbf{F}_{n,\alpha\beta} + \mathbf{F}_{t,\alpha\beta}, \tag{12}$$

where $\mathbf{F}_n$ and $\mathbf{F}_t$ are the normal and tangential forces acting at the contact point C (Fig. 1).

When the rolling friction is neglected, the particle's torque moment due to the tangential force $\mathbf{F}_{t,\alpha\beta}$ is defined as follows

$$\mathbf{M}_{\alpha\beta} = \mathbf{F}_{t,\alpha\beta} \times \mathbf{d}_{C,\alpha\beta}, \tag{13}$$

where the vector $\mathbf{d}_{C,\alpha\beta}$ is defined in (8).

In the DEM, the evaluation of interaction forces takes most of the modelling time [23, 24]. Therefore, the choice of the interaction law is not unique and requires compromise between both model accuracy and its simplicity.

In the present article, our focus is on capturing the stick-sliding behaviour; therefore, a relatively hard contact model is considered. We assume full stick of particles without micro-slip and neglect viscous damping. Consequently, contact behaviour in normal direction is assumed to be elastic and described by the Hertz contact law, and elastic-frictional in the tangential direction. The contact model under consideration can be represented by the normal non-linear elastic spring having stiffness k_n and by the tangential incrementally linear elastic spring with stiffness k_t combined with the slider block (Fig. 2).

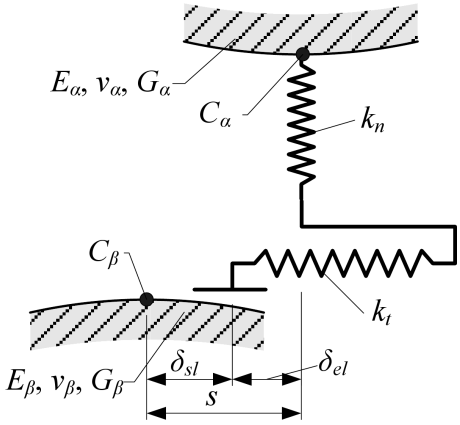

Fig. 2. A schematic view of the particle-particle or particle-wall interaction

The normal elastic contact is described according to Hertz model. It can be expressed in terms of the normal repulsive force $\mathbf{F}_n$ and the overlap h

$$\mathbf{F}_{n,\alpha\beta} = \mathbf{n}\int_0^h k_n\left(h\right)dh = \mathbf{n}4/3E^{\mathit{eff}}\sqrt{R^{\mathit{eff}}}h^{(3/2)}. \tag{14}$$

Here, the normal interaction stiffness k_n is nonlinear and depends on the overlap h

$$k_n\left(h\right) = 2E^{\mathit{eff}}\sqrt{R^{\mathit{eff}}}\sqrt{h}, \tag{15}$$

where R^{eff} is the effective radius representing the radii of the contacting particles

$$R^{\mathit{eff}} = \frac{R_\alpha R_\beta}{R_\alpha + R_\beta}. \tag{16}$$

In the case of the particle-wall interaction, when the wall radius $R_w = \infty$, then, $R^{\mathit{eff}} = R_\alpha$ where R_α is the radius of the particle.

In Eq. (15), E^{eff} stands for the effective elastic modulus

$$E^{\mathit{eff}} = \frac{E_\alpha E_\beta}{E_\alpha\left(1-\nu_\beta^2\right) + E_\beta\left(1-\nu_\alpha^2\right)}, \tag{17}$$

where $\alpha,\beta \in \{i,j,w\}$, while v stands for Poison's ratios of the particles.

The tangential elastic-frictional contact is much more complex. We assume that, in the tangential direction colliding objects interact according to the regularised dry friction Coulomb law

$$\mathbf{F}_t = \begin{cases} 0, & \text{when } \mathbf{F}_n = 0 & \text{no contact} \\ \mathbf{F}_{t,st}, & \text{when } \|\mathbf{F}_{t,st}\| < \mu\mathbf{F}_n & \text{contact with stick} \\ \mathbf{F}_{t,sl}, & \text{when } \|\mathbf{F}_{t,sl}\| = \mu\mathbf{F}_n & \text{contact with slip} \end{cases} \tag{18}$$

where $\mathbf{F}_{t,st}$ and $\mathbf{F}_{t,sl}$ represent the so-called stick force and sliding frictional force, respectively

$$\mathbf{F}_{t,sl} = \mathbf{t}\mu||\mathbf{F}_n||, \tag{19}$$

where μ is the coefficient of friction.

Let us consider the tangential contact more carefully. Let the particle α moves with respect to the β particle. If the Coulomb limit is not reached, then, really, the contact points

C_α and C_β do not move with respect to each other. This contact mode is called the stick mode in present article. In this case, the elastic deformation of the particles leads to the relative displacement of the particles' points that do not belong to the contact area. Let tangential relative elastic displacement of the centres of the particles α and β be represented by elongation of the elastic spring with stiffness k_t (Fig. 2). When the Coulomb limit is reached, the contact points C_α and C_β move due to the so-called gross sliding or block slip. This mode is called sliding mode. The stick or sliding modes of the contact point C, $C \in \{C_\alpha, C_\beta\}$, may be interpreted based on the elastoplastic analogy of the friction models via a sliding surface formulation, see Michalowski and Mróz [25] and Wriggers [26]. Thus, the tangential motion of the contact point C may be decomposed into the elastic and irreversible sliding parts characterized by the displacements $\boldsymbol{\delta}_{el}$ and $\boldsymbol{\delta}_{sl}$, respectively. As a result, the total tangential displacement $\mathbf{s}$ of the contact point C reads as

$$\mathbf{s}(t) = \boldsymbol{\delta}_{el}(t) + \boldsymbol{\delta}_{sl}(t). \tag{20}$$

In general, there are two approaches to calculate the tangential force: non-incremental and incremental ones. These different approaches were studied numerically by Thornton [7] and Kruggel-Emden [10]. These authors provided a numerical example to show that the non-incremental formula is not suitable when the tangential stiffness is not constant during the contact.

The incremental formulation is given in the Subsec. 3.1. The non-incremental formula is as follows

$$\mathbf{F}_{t,st}(t) = -k_t(t)\boldsymbol{\delta}_{el}(t). \tag{21}$$

The tangential stiffness k_t is nonlinear with respect to the overlap h. According to Kohring [27] k_t is given by the following formula

$$k_t(t) = 8G^{\mathit{eff}}\sqrt{R^{\mathit{eff}}}\sqrt{h(t)}, \tag{22}$$

where G^{eff} is the equivalent shear modulus of the materials of two particles

$$G^{\mathit{eff}} = \frac{2}{3}\frac{G_\alpha G_\beta}{G_\alpha\,(2-\nu_\beta) + G_\beta\,(2-\nu_\alpha)}. \tag{23}$$

The time integration of the velocity from the beginning of the contact ($t_{c,0}$) yields the total tangential displacement (Fig. 2) denoted hereafter by $\mathbf{s}(t)$

$$\mathbf{s}(t) = \int_{t_{c,0}}^{t} \mathbf{v}_{C,t}(\tau)d\tau. \tag{24}$$

Since $\mathbf{s}$ is defined, the sliding displacement of contact point may be defined from the expression (20) as follows

$$\boldsymbol{\delta}_{sl}(t) = \mathbf{s}(t) - \boldsymbol{\delta}_{el}(t). \tag{25}$$

3. Description of tangential contact

3.1. Incremental methodology for evaluating the tangential contact. The incrementally linear approach for evaluation of the tangential elastic displacement δ_{el} is presented in this section. This approach is compatible with the explicit time integration of the equations of the motion. It is established, however, that the force-displacement relationship depends on both the tangential and normal loading history. Possible sliding of a particle, which may appear in both coincident and opposite directions with respect to the applied tangential force or displacement, leads to numerically sensitive complications.

The time-dependent, incrementally linear tangential constitutive relationship may be expressed applying a vector-valued functional at the beginning of the contact, i.e. $t = t_{c,0}$. When the displacement-driven approach, typical for the DEM, is used, the tangential stick force $\mathbf{F}_{t,st}$ is as follows

$$\mathbf{F}_{t,st}(t_m) = -\int_{t_{c,0}}^{t_m} k_t(\tau t)\frac{d\boldsymbol{\delta}_{el}(\tau)}{d\tau}d\tau. \tag{26}$$

In (26), $\mathbf{F}_{t,st}$ can be treated as a linear functional. If the stiffness k_t is constant during the contact, i.e. $k_t(t)$ = constant as $t \in [t_{m-1}, t_m]$, then the solution of Eq. (26) is Eq. (21). Integral (26) can be calculated numerically by applying incremental approach. It should be noticed that even more sophisticated approaches with the so-called fractional derivatives, whose order are not integer but rational positive number, can be applied to model the contact problem of the particles, Leszczynski [28]. For the time increment Δt considered between time instants t_{m-1} and t_m, integral (26) may be expressed in the incremental form as follows

$$\mathbf{F}_{t,st}\,(t_m) = \mathbf{F}_{t,st}\,(t_{m-1}) + \Delta\mathbf{F}_{t,st}\,(t_m)\,, \tag{27}$$

where $\Delta\mathbf{F}_{t,st}(t_m)$ is the increment of the tangential force

$$\Delta\mathbf{F}_{t,st}\,(t_m) = -\int_{t_{m-1}}^{t_m} k_t\,(\tau)\,\frac{d\boldsymbol{\delta}_{el}\,(\tau)}{d\tau}d\tau. \tag{28}$$

There are many methods for calculating the integral (28). The simplest way is to use a rectangular approximation of the stiffness k_t with the constant value during the time increment Δt. The stiffness can be taken as an arbitrary point $k_t(\xi) \in [k_t(t_{m-1}),\, k_t(t_m)]$

$$k_t\,(\xi) = k_t(t_{m-1}) + (k_t\,(t_m) - k_t\,(t_{m-1}))\,\eta, \tag{29}$$

where $\eta \in [0, 1]$.

As simple approaches, the following approximations of the stiffness k_t can be used:
the backward approximation, when the left-end point is taken

$$k_t\,(\xi) = k_t\,(t_{m-1})\,, \tag{30}$$

the forward approximation, when the right-end point is taken

$$k_t\,(\xi) = k_t\,(t_m)\,, \tag{31}$$

or the average approximation, when the midpoint is taken

$$k_t\,(\xi) = (k_t\,(t_m) + k_t\,(t_{m-1}))/2. \tag{32}$$

It should be emphasized that the forward approximation has an advantage over other rules because there is no need to store the information of the previous step in the computer memory.

When the rectangular approximation is applied to the force increment, in the integral (28), then Eq. (27) can be rewritten as follows

$$\begin{aligned}\mathbf{F}_{t,st}\left(t_m\right) &= \mathbf{F}_{t,st}\left(t_{m-1}\right) \\ &- k_t\left(\xi\right)\left(\boldsymbol{\delta}_{el}\left(t_m\right) - \boldsymbol{\delta}_{el}\left(t_{m-1}\right)\right).\end{aligned} \tag{33}$$

It should be emphasized that the displacement-driven approach used in the general Eq. (28) or the incremental Eq. (33) is convenient to calculate the tangential stick force $\mathbf{F}_{t,st}$, when the tangential elastic displacement $\boldsymbol{\delta}_{el}$ is already known.

Equation (33) can be solved with respect to the displacement $\boldsymbol{\delta}_{el}$. The solution is as follows

$$\begin{aligned}\boldsymbol{\delta}_{el}\left(t_m\right) &= \boldsymbol{\delta}_{el}\left(t_{m-1}\right) \\ -\frac{1}{k_t\left(\xi\right)}&\left(\mathbf{F}_{t,st}\left(t_m\right) - \mathbf{F}_{t,st}\left(t_{m-1}\right)\right).\end{aligned} \tag{34}$$

If the Coulomb limit is reached, $\mathbf{F}_{t,st}(t_m) = \mathbf{t}\mu||\mathbf{F}_n(t_m)||$, we get the incremental formula for recalculation of the elastic displacement

$$\begin{aligned}\boldsymbol{\delta}_{el}\left(t_m\right) &= \boldsymbol{\delta}_{el}\left(t_{m-1}\right) \\ -\frac{1}{k_t\left(\xi\right)}&\left(\mathbf{t}\mu\left\|\mathbf{F}_n\left(t_m\right)\right\| - \mathbf{F}_t\left(t_{m-1}\right)\right).\end{aligned} \tag{35}$$

However, another form of the integral equation using the force-driven approach can be more convenient to calculate the displacement $\boldsymbol{\delta}_{el}$, when the force $\mathbf{F}_t$ is known. It could be also expressed as the vector-valued functional

$$\boldsymbol{\delta}_{el}\left(t_m\right) = -\int_{t_{c,0}}^{t_m} \frac{1}{k_t\left(\tau\right)}\frac{d\mathbf{F}_t\left(\tau\right)}{d\tau}d\tau. \tag{36}$$

The incremental approach applied to integral (36) is as follows

$$\boldsymbol{\delta}_{el}\left(t_m\right) = \boldsymbol{\delta}_{el}\left(t_{m-1}\right) - \int_{t_{m-1}}^{t_m} \frac{1}{k_t\left(\tau\right)}\frac{d\mathbf{F}_t\left(\tau\right)}{d\tau}d\tau, \tag{37}$$

where $\mathbf{F}_t \in \{\mathbf{F}_{t,st},\ \mathbf{t}\mu||\mathbf{F}_n||\}$ is defined in Eq. (18), $\mathbf{F}_{t,st}$ is given in Eq. (27). If the identical incremental procedure with the constant value of the stiffness $k_t(\xi)$, Eq. (29), during the current increment Δt, were applied for Eq. (37), then the Eq. (35) would be obtained.

In the DEM, it is generally agreed that the integral (24) is calculated using an incremental approach

$$\mathbf{s}\left(t_m\right) = \mathbf{s}\left(t_{m-1}\right) + \Delta\mathbf{s}\left(t_m\right), \tag{38}$$

where $\Delta\mathbf{s}\left(t_m\right) = \int_{t_{m-1}}^{t_m} \mathbf{v}_{C,t}\left(\tau\right)d\tau \approx \mathbf{v}_{C,t}\left(t_m\right)\Delta t.$

In the case, when the Coulomb limit is not reached at the time instant t_m, the elastic component of the tangential displacement (Fig. 2) may be defined basing on the expression (38)

$$\boldsymbol{\delta}_{el}\left(t_m\right) = \boldsymbol{\delta}_{el}\left(t_{m-1}\right) + \Delta\boldsymbol{\delta}_{el}\left(t_m\right), \tag{39}$$

where $\Delta\boldsymbol{\delta}_{el}(t_m) = \Delta\mathbf{s}(t_m)$. This formula is frequently applied in DEM simulation.

The rectangular approximation of the stiffness $k_t(t)$, with $t \in [t_{m-1}, t_m]$, can be treated as the generalized mean of the integral (28)

$$\begin{aligned}k_t\left(\xi\right) &= \frac{\left\|\int_{t_{m-1}}^{t_m} k_t\left(\tau\right)\frac{d\boldsymbol{\delta}_{el}\left(\tau\right)}{d\tau}d\tau\right\|}{\left\|\int_{t_{m-1}}^{t_m}\frac{d\boldsymbol{\delta}_{el}\left(\tau\right)}{d\tau}d\tau\right\|} \\ &= \frac{\left\|\Delta\mathbf{F}_{t,st}\left(t_m\right)\right\|}{\left\|\boldsymbol{\delta}_{el}\left(t_m\right) - \boldsymbol{\delta}_{el}\left(t_{m-1}\right)\right\|}.\end{aligned} \tag{40}$$

For the mean value $k_t(\xi)$, the inequality $(\min k_t(t)) \le k_t(\xi) \le (\max k_t(t))$ holds as $t \in \{t_{m-1}, t_m\}$. If $k_t(t)$ is a monotonic function on the interval $[t_{m-1},\ t_m]$ and $k_t(t_{m-1}) \le k_t(t_m)$, then the following inequality is valid for the increment of the stick force $\mathbf{F}_{t,st}$

$$\begin{aligned}k_t\left(t_{m-1}\right)\left\|\Delta\boldsymbol{\delta}_{el}\left(t_m\right)\right\| &\le \left\|\Delta\mathbf{F}_{t,st}\left(t_m\right)\right\| \\ &\le k_t\left(t_m\right)\left\|\Delta\boldsymbol{\delta}_{el}\left(t_m\right)\right\|,\end{aligned}$$

where $\Delta\mathbf{F}_{t,st}$ and $\Delta\boldsymbol{\delta}_{el}(t_m)$ are defined in (28) and (39), (38) or $\Delta\boldsymbol{\delta}_{el}(t_m) = (\boldsymbol{\delta}_{el}(t_{m-1}) - \boldsymbol{\delta}_{el}(t_m))$.

It could be summarized, that in the case of stick mode the behaviour of the contact could be defined incrementally by tracing the loading history according to Eqs. (27) or (33), where evaluation of the displacement $\boldsymbol{\delta}_{el}$ requires solution of the integral equation (26) or (27) together with (28). This approach is termed hereafter as displacement-driven approach. Alternatively, contact behaviour could be defined by tracing incrementally the displacement history according to (37), where evaluation of the tangential force $\mathbf{F}_t$ requires solution of the integral equation (36).

For the clarity sake the algorithm for the calculation of the parameters of the tangential interaction, including newly elaborated method for calculation of the tangential elastic displacement $\boldsymbol{\delta}_{el}$, is represented in the form of a flowchart in Fig. 3.

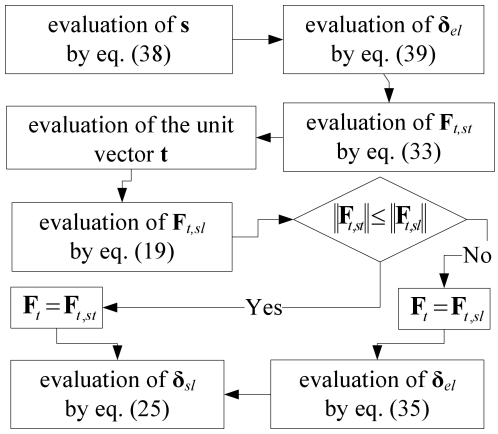

Fig. 3. The block scheme of the algorithm for calculation of the interaction parameters

3.2. Analytical comparison of proposed and existing methodologies. According to existing DEM methodology, see for example [10, 14, 15, 17, 21], when the Coulomb limit is exceeded the tangential displacement $\boldsymbol{\delta}_{el}$ is recalculated as follows

$$\boldsymbol{\delta}_{el}\left(t_m\right) = -\frac{\mathbf{t}\mu \left\|\mathbf{F}_n\left(t_m\right)\right\|}{k_t\left(t_m\right)}. \tag{41}$$

It is evident that the standard formula (41) is obtained by using the non-incremental equation (21), when $\mathbf{F}_{t,st} = \mathbf{t}\mu||\mathbf{F}_n)||$. As it is demonstrated above (after Eq. (26)), the non-incremental Eq. (21) is valid, when the tangential stiffness is constant during the contact. Therefore, the standard Eq. (41) is valid only if the tangential stiffness k_t is constant during the contact. The proposed solutions, (35) and (37), do not have this restriction.

This section presents theoretical comparison of the stick tangential force $\mathbf{F}_{t,st}$ obtained for the tangential elastic displacement $\boldsymbol{\delta}_{el}$ calculated according to the conventional (41) and newly elaborated (35) approaches. The formula (33) for the stick force $\mathbf{F}_{t,st}$ includes elastic displacement $\boldsymbol{\delta}_{el}(t)$, $t \in \{t_m, t_{m-1}\}$, which is different depending on which approach, conventional (41) or newly elaborated (35) one, is used when the Coulomb limit is reached. Therefore, there is reason to compare $\mathbf{F}_{t,st}$ when it is calculated taking $\boldsymbol{\delta}_{el}$ according to different formulas (41) and (35). For the sake of clarity the conventional approach is described by expressions (42) and denoted hereafter by the upper subscript I. The newly elaborated and developed by the authors approach is described by expressions (43) and denoted hereafter by the upper subscript II. Thus, the evaluation of the displacement may be summarised as follows

$$\boldsymbol{\delta}^{I}_{el}(t_m) = \begin{cases} \boldsymbol{\delta}^{I}_{el}\left(t_{m-1}\right) + \displaystyle\int_{t_{m-1}}^{t_m} \mathbf{v}_{C,t}(\tau)d\tau, \\ \qquad \text{when } ||\mathbf{F}_{t,st}|| \le \mu||\mathbf{F}_n|| \\ \mathbf{t}\dfrac{\mu||\mathbf{F}_n(t_m)||}{k_t(\xi)}, \text{ when } ||\mathbf{F}_{t,st}|| > \mu||\mathbf{F}_n|| \end{cases} \tag{42}$$

$$\boldsymbol{\delta}^{II}_{el}(t_m) = \begin{cases} \boldsymbol{\delta}^{II}_{el}\left(t_{m-1}\right) + \displaystyle\int_{t_{m-1}}^{t_m} \mathbf{v}_{C,t}(\tau)d\tau, \\ \qquad \text{when } ||\mathbf{F}_{t,st}|| \le \mu||\mathbf{F}_n|| \\ \boldsymbol{\delta}^{II}_{el}\left(t_{m-1}\right) - \dfrac{1}{k_t(\xi)}(\mathbf{t}\mu||\mathbf{F}_n(t_m)|| - \mathbf{F}_t(t_{m-1})), \\ \qquad \text{when } ||\mathbf{F}_{t,st}|| > \mu\mathbf{F}_n|| \end{cases} \tag{43}$$

where $\mathbf{F}_t$ and $\mathbf{F}_{t,st}$ are calculated according to Eqs. (18) and (27) or (33), and $\mathbf{v}_{C,t}$ is calculated according to Eq. (11).

Let us compare δ_{el} given in Eqs. (35) and (41), when the Coulomb limit is reached, i.e. when $||\mathbf{F}_{t,st}|| > \mu||\mathbf{F}_n||$, by taking the difference $\boldsymbol{\delta}^{II}_{el} - \boldsymbol{\delta}^{I}_{el}$

$$\boldsymbol{\delta}^{II}_{el}(t_m) - \boldsymbol{\delta}^{I}_{el}(t_m) = \frac{\mathbf{F}_t\left(t_{m-1}\right)}{k_t\left(\xi\right)} + \boldsymbol{\delta}^{II}_{el}\left(t_{m-1}\right). \tag{44}$$

In one-dimensional case $\mathbf{F}_t(t_{m-1})$ and $\boldsymbol{\delta}_{el}(t_m)$ are the opposite vectors. Therefore, it can be seen from Eq. (44), that $||\boldsymbol{\delta}^{II}_{el}(t_m)||$ is bigger than $||\boldsymbol{\delta}^{I}_{el}(t_m)||$ when $\left\|\boldsymbol{\delta}^{II}_{el}\left(t_{m-1}\right)\right\| - \left\|\mathbf{F}_t\left(t_{m-1}\right)\right\|/k_t\left(\xi\right) > 0$.

Let us show that the force $\mathbf{F}_{t,st}$ calculated according to Eq. (33) by taking $\boldsymbol{\delta}_{el} = \boldsymbol{\delta}^{I}_{el}$ and $\boldsymbol{\delta}_{el} = \boldsymbol{\delta}^{II}_{el}$ is the same. If the Coulomb limit is not reached from the beginning of the contact, then the force $\mathbf{F}_{t,st}$ calculated using $\boldsymbol{\delta}^{I}_{el}$ or $\boldsymbol{\delta}^{II}_{el}$ is the same because $\boldsymbol{\delta}^{I}_{el} = \boldsymbol{\delta}^{II}_{el}$ and $\mathbf{F}_t = \mathbf{F}_{t,st}$. However, as it is shown in (44), if the Coulomb limit is reached, then δ^{I}_{el} and $\boldsymbol{\delta}^{II}_{el}$ are different. Let we show now that $\mathbf{F}_{t,st}$ calculated according to Eq. (33) taking $\boldsymbol{\delta}_{el} = \boldsymbol{\delta}^{I}_{el}$ and $\boldsymbol{\delta}_{el} = \boldsymbol{\delta}^{II}_{el}$ is the same when the Coulomb limit is reached. Let $\mathbf{F}_{t,st}$ calculated from Eq. (33) be $\mathbf{F}^{I}_{t,st}$ and $\mathbf{F}^{II}_{t,st}$ when $\boldsymbol{\delta}_{el} = \boldsymbol{\delta}^{I}_{el}$ and $\boldsymbol{\delta}_{el} = \boldsymbol{\delta}^{II}_{el}$, respectively, and let $k_t(\xi)$ be the same for $\boldsymbol{\delta}^{I}_{el}$ and $\boldsymbol{\delta}^{II}_{el}$. Then from Eq. (33), we see that $\mathbf{F}^{I}_{t,st}$ and $\mathbf{F}^{II}_{t,st}$ are different only if the differences $\Delta\boldsymbol{\delta}^{i}_{el}(t_m) = \boldsymbol{\delta}^{i}_{el}(t_m) - \boldsymbol{\delta}^{i}_{el}(t_{m-1}) i \in \{I, II\}$ are different i.e. only if $\Delta\boldsymbol{\delta}^{I}_{el}(t_m) \neq \Delta\boldsymbol{\delta}^{II}_{el}(t_m)$. The elastic displacement $\boldsymbol{\delta}^{i}_{el}(t_m)$ is calculated according to Eq. (39); therefore, the differences $\Delta\boldsymbol{\delta}^{i}_{el}(t_m) = \boldsymbol{\delta}^{i}_{el}(t_{m-1}) + \Delta\mathbf{s}(t_m) - \boldsymbol{\delta}^{i}_{el}(t_{m-1}) = \Delta\mathbf{s}(t_m), i \in \{I, II\}$. That is, $\Delta\boldsymbol{\delta}^{I}_{el}(t_m) = \Delta\boldsymbol{\delta}^{II}_{el}(t_m) = \Delta\boldsymbol{\delta}_{el}(t_m) = \Delta\mathbf{s}(t_m)$. Hence, the tangential forces $\mathbf{F}_{t,st}$ given by Eq. (33) are the same when $\boldsymbol{\delta}^{I}_{el}$ and $\boldsymbol{\delta}^{II}_{el}$ are taken according to Eqs. (42) and (43). The algorithm elaborated for tracking of the tangential behaviour is presented in Fig. 3 and Appendix.

3.3. On verification of zero velocity. This section gives a method for calculating the time when the relative velocity of the contact point equals zero during the contact i.e. when the condition $\mathbf{v}_{C,t} = 0$ holds. It may be necessary for analysis of the particle interaction. The expression for the tangential component of the relative velocity ($\mathbf{v}_{C,t,\alpha\beta}$) at the contact point is given in Eq. (11). Using constant integration step size it is impossible to verify if $\mathbf{v}_{C,t} = 0$. Therefore, the verification of the condition $\mathbf{v}_{C,t} = 0$ requires an extra calculation.

The method for evaluation of the condition $\mathbf{v}_{C,t} = 0$ during the considered integration step $(t_{m-1}, t_m]$ can be as follows. Let at the considered instant time t_m the relative velocity $\mathbf{v}_{C,t}(t_m)$ be known. Using the values $\mathbf{v}_{C,t}(t_{m-2})$, $\mathbf{v}_{C,t}(t_{m-1})$, $\mathbf{v}_{C,t}(t_m)$ the time t_ξ is calculated when the equality $\mathbf{v}_{C,t}(t_\xi) = 0$ holds. If the obtained t_ξ satisfies the condition $t_{m-1} < t_\xi \le t_m$, then the condition $\mathbf{v}_{C,t} = 0$ is realized during the considered integration step $(t_{m-1}, t_m]$, and we can take $\mathbf{v}_{C,t} = 0$ at the time t_m.

One method to calculate the time t_ξ when $\mathbf{v}_{C,t}(t_\xi) = 0$ is suggested by Zhang and Whiten [29]. After rearrangement, their formula can be expressed as follows

$$t_\xi = t_{m-1} + \frac{v_{C,t}\left(t_m\right)}{\mu\left\|\mathbf{F}_n\left(t_m\right)\right\| H}, \tag{45}$$

where

$$H = \left(\frac{1}{m_i} + \frac{\left\|\mathbf{d}_{C,ij}\right\|^2}{I_i} + \frac{1}{m_j} + \frac{\left\|\mathbf{d}_{C,ji}\right\|^2}{I_j}\right).$$

It should be noted that the suggested formula has two disadvantages. Firstly, it is suitable only when the Coulomb limit is reached, and secondly, there is indeterminacy because of

scalar value of the relative velocity $v_{C,t}$ in Eq. (45). Therefore, we developed another formula for calculation of t_ξ

$$t_\xi = t_{m-1} + \frac{\|\mathbf{v}_{C,t}(t_m)\|}{-F_{t,proj}(t_m)\,H}, \tag{46}$$

where $F_{t,proj}(t_m)$ is projection of the tangential force vector $\mathbf{F}_t(t_m)$ onto the relative velocity vector $\mathbf{v}_{C,t}(t_m)$

$$F_{t,proj}(t) = proj_{\mathbf{v}_{C,t}(t_m)}\mathbf{F}_t(t_m) = \frac{\mathbf{v}_{C,t}(t_m) \bullet \mathbf{F}_t(t_m)}{\|\mathbf{v}_{C,t}(t_m)\|}. \tag{47}$$

It is also possible to verify whether $\mathbf{v}_C(t_\xi) = 0$ when $t_\xi \in (t_{m-1}, t_m]$ by using the projection $\mathbf{v}_{C,t}(t_m)$ onto $\mathbf{v}_{C,t}(t_{m-1})$

$$pr = proj_{\mathbf{v}_{C,t}(t_{m-1})}\mathbf{v}_{C,t}(t_m) = \frac{\mathbf{v}_{C,t}(t_{m-1}) \bullet \mathbf{v}_{C,t}(t_m)}{\|\mathbf{v}_{C,t}(t_{m-1})\|}. \tag{48}$$

If $pr \geq 0$, then the projection of $\mathbf{v}_{C,t}(t_m)$ onto $\mathbf{v}_{C,t}(t_{m-1})$ has the same direction, and as a result the condition $\mathbf{v}_{C,t}(t_\xi) = 0$ is not realized during the integration step $(t_{m-1},\ t_m]$. If $pr < 0$, then, the projection of $\mathbf{v}_{C,t}(t_m)$ onto $\mathbf{v}_{C,t}(t_{m-1})$ is opposite, and as a result, the condition $\mathbf{v}_{C,t}(t_\xi) = 0$ is realized during the integration step $(t_{m-1},\ t_m]$.

4. Numerical analysis and results

The oblique impact of an elastic spherical particle on an elastic infinite half space was investigated (Fig. 4) applying the conventional (42) and newly developed (43) approximations, as well as using three versions of direction vector in Eq. (19).

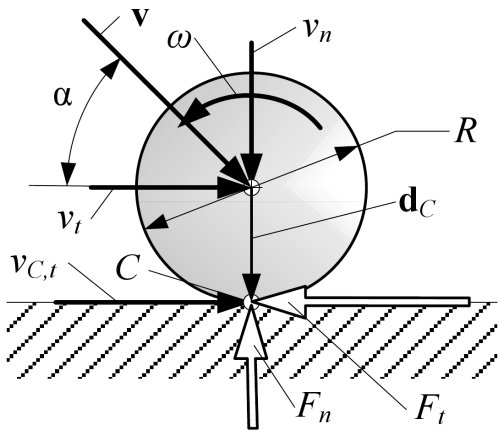

Fig. 4. The oblique impact scheme

The spherical particle is characterised by the radius $R = 5$ cm, elastic modulus E equal to 0.3 GPa and Poison's ratio ν equal to 0.3. The material density is assumed equal to 1000 kg/m^3, thus the particle mass is $m = 1/6\pi \approx 5.236$ kg. The tangential friction coefficient is $\mu = 0.3$. The elastic modulus E_w and Poison's ratio ν_w of the target wall are equal to those of the particle. The geometry of contact and initial data are shown in Fig. 4. Initial position of the particle indicates contact occurring at the point C. The initial conditions of the particle are specified by the impact velocity $v = 0.201$ m/s and attack angle $\alpha = 1.471$ (normal and tangential velocities: $v_y = 0.2$ m/s and $v_x = 0.02$ m/s) as well as the angular velocity $\omega = 3.6$ rad/s. The time step length for the time integration was estimated by taking 51 steps for the contact interval.

A series of the numerical tests were conducted to investigate the stick-sliding behaviour of the particle. The tests will illustrate the importance of our developments and their influence on the evaluated parameters.

4.1. The analysis of the stick-slip condition. The first test illustrates the nature and complexity of the elastic-frictional tangential contact under variable normal load. On the other hand, simulation results reflect the capability and quality of the newly developed calculation method. Thus, by tracing contact behaviour in time we will show advantages of the suggested method (35) or (43) over the conventional one. It should be noted that the tangential unit vector t in (19) is considered on the basis of the force-driven methodology by tracking the direction of the tangential force, i.e. $\mathbf{t} = \mathbf{F}_{t,st}/||\mathbf{F}_{t,st}||$. The sample data was selected from a series of numerical experiments aimed to illustrate possible situations and variety of motion modes.

The almost standard oblique impact test is used to illustrate the influence of the variable normal load on the interaction parameters. The time t is normalized with respect to the duration of the contact $t_c^* = (t - t_{c,0})/t_{c,dur}$ where $t_{c,0}$ is the time at the beginning of the contact and $t_{c,dur}$ is the duration of the contact. The normal force F_n, and normal and tangential stiffnesses k_n and k_t are normalized with respect to its maximal values. That is, $F_n^* = F_n/\max\{F_n\}$, $k_i^* = k_i/\max\{k_i\}$, here $i \in \{n, t\}$. It is evident that these normalized variables vary within the interval [0,1]. The characteristic simulation results with respect to the normalized contact time t^* are presented in Fig. 5. The parameters given there were calculated with $\boldsymbol{\delta}_{el} = \boldsymbol{\delta}_{el}^{II}$, and $\boldsymbol{\delta}_{el}^{II}$ was calculated according to Eq. (43).

The behaviour of the normal contact is shown in Fig. 5a, where all variables are normalised. The normalized normal force F_n^* and normalized stiffnesses k_n^* and k_t^* vary in the range between 0 and 1 and are depicted in Fig. 5a. The normal contact variables are independent on the tangential contact. It should be noted that the normalized curves k_n^* and k_t^* in Fig. 5 coincide because the stiffness ratio k_t/k_n depends only on Poison's ratio; hence, k_t/k_n = const during the contact when the tangential and normal interaction stiffness parameters are given by Eqs. (15) and (22). If k_n and k_t differ only by a constant, then $k_n^* = k_t^*$.

The variations of the tangential and normal variables, i.e. displacements, forces and velocities are presented in Fig. 5a,b,c, respectively. Figure 5b shows tangential displacements, i.e. elastic component (spring elongation) δ_{el} and sliding component δ_{sl} as well as the total tangential displacement of the contact point of the particle $s = \delta_{el} + \delta_{sl}$. The normal velocities of the particle centre v_n and the contact point $v_{C,n}$, as well as the tangential velocity $v_{C,t}$ of the contact point C are depicted in Fig. 5c to illustrate the influence of the rotation. The tangential force F_t of the particle contact point and difference $F_t - \mu||F_n||$ are depicted in Fig. 5d.

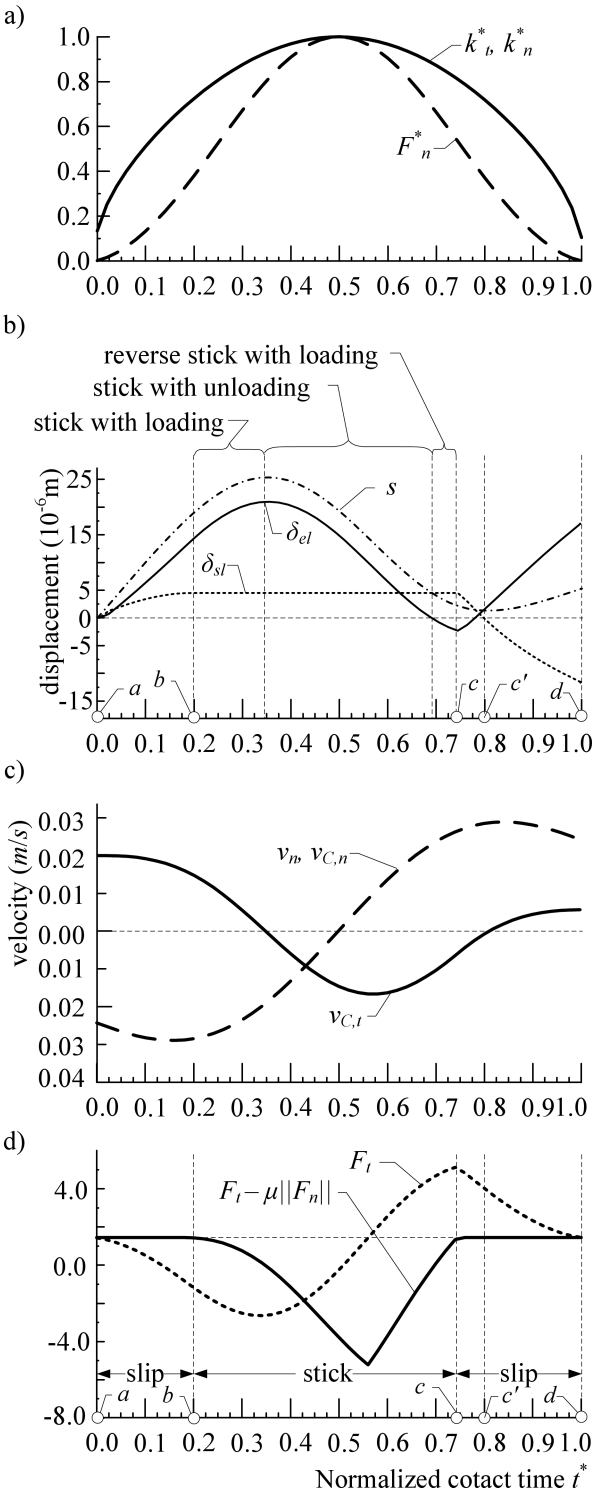

Fig. 5. The dependences of the interaction parameters of the particle's contact point on the normalized contact time t^* during the first contact: a) normalized normal force F_n^* and normalized stiffnesses k_n^* and k_t^*, b) displacements and modes of the interaction, c) tangential $v_{C,t}$ and normal v_n velocities, d) tangential force F_t and difference $F_t - \mu||F_n||$

Various particle-plane interaction modes could be observed during impact. Variation of the forces (Fig. 5d) indicates stick-slip-stick modes, while variation of displacements (Fig. 5b) gives additional information about modes of the particle motion. Five particle-plane interaction modes, namely, slip, elastic stick with loading, elastic stick with unloading, reverse elastic stick with reloading and slip occur during the first contact before rebounding (Fig. 5b,d).

The time instants when different contact mode switches are depicted with points a–d. The segment between points a and b illustrates sliding behaviour, between points b and c illustrates stick behaviour, between c and d illustrates again sliding behaviour. In Fig. 5b and d the time when the condition $\mathbf{v}_{C,t} = 0$ is realized is denoted by point c'.

4.2. Investigation of the tangential elastic displacement of the contact point. Time dependence of the tangential elastic displacement of the contact point of the considered particle obtained in calculations according to Eq. (43) and standard Eq. (42) is shown in Fig. 6a. As we can see, according to the standard method, the artificial jump is clearly indicated in stick-sliding transition point. According to the our approach given by Eq. (43) no artificial jump occurs in the $\boldsymbol{\delta}_{el} - t$ relationship.

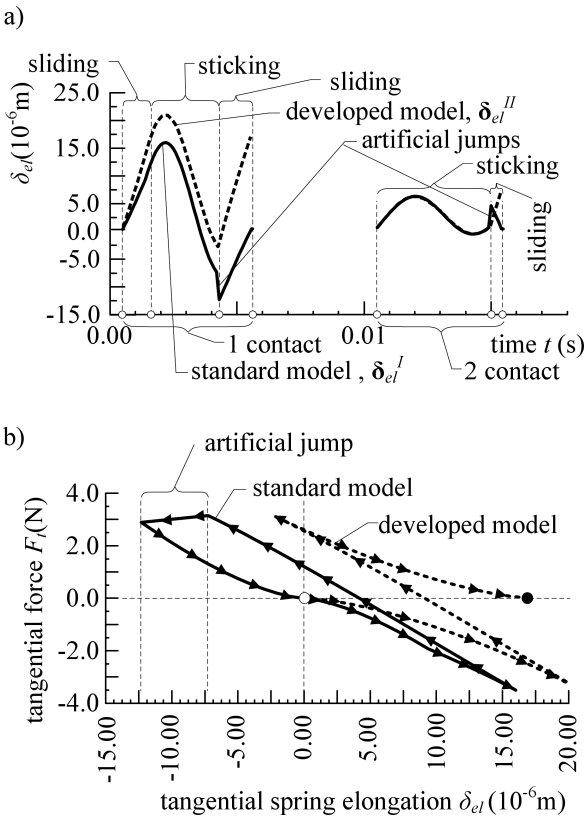

Fig. 6. The dependences of the contact point interaction parameters: a) tangential elastic displacement δ_{el} during the two contacts, b) tangential force F_t during the first contact

The curves showing the dependence of the tangential force F_t on the tangential elastic displacement δ_{el} according to the proposed (43) and standard (42) formulas during the first contact are given in Fig. 6b. The beginning and end of the contact are denoted by the symbols ○ and ●, respectively. As we can

see from the Fig. 6b the behaviour of the tangential elastic displacement obtained according to the proposed formula (43) is different from that predicted by the standard equation (42). According to the newly proposed method (43), the tangential elastic displacement is not equal zero at the end of contact, while according to the standard method (42), the tangential elastic displacement equals zero at the end of the contact. As it can be seen from Fig. 6, according to the standard method the artificial jump is clearly indicated at the stick-sliding transition point in δ_{el}^{I}-t and F_t-δ_{el} diagrams. At the transition point stick changes into slip, or condition $||\mathbf{F}_t|| \leq \mu||\mathbf{F}_n||$ changes into condition $|\mathbf{F}_t|| = \mu||\mathbf{F}_n||$. According to the proposed Eq. (43) no artificial jump occurs in the δ_{el}^{II}-t relationship. The discontinuity at the transition point can be treated as discontinuity of the first kind like in mathematical analysis. The proposed solution (43) does not have this disadvantage. These differences between the proposed and standard method show that the proposed methodology for calculation of $\boldsymbol{\delta}_{el}$ allows us to analyse more accurately the parameters of the tangential interaction, namely the elastic $\boldsymbol{\delta}_{el}$ and sliding $\boldsymbol{\delta}_{sl}$ displacements.

5. Investigation of the unit vector t

Evaluation of the tangential behaviour is complicated not only from a theoretical point of view but even more because of complications in the numerical implementation. Based on the programming experience and literature analysis, it could be stated that keeping the orthogonally of the basis of the local coordinate frame during the entire contact duration is a complicated task. More precisely, the problem concerns evaluation of the unit vector $\mathbf{t}$ in the tangential direction. Even analysis of the literature shows that the solution is non-unique.

Three approaches for calculation of the tangential direction vector $\mathbf{t}$ when the Coulomb limit is reached have been found in the references. The most popular is the velocity-driven approach, where the tangent direction $\mathbf{t} = -\mathbf{v}_{C,t}/||\mathbf{v}_{C,t}||$ is determined by the tangential component of the relative velocity $\mathbf{v}_{C,t}$ at the contact point [17–19]. The displacement-driven approach employs the direction of the elastic tangential displacement, thus $\mathbf{t} = -\boldsymbol{\delta}_{el}/||\boldsymbol{\delta}_{el}||$ [14], while the force-driven approach employs the direction of the tangential force $\mathbf{F}_t$, namely: $\mathbf{t} = \mathbf{F}_{t,st}/||\mathbf{F}_{t,st}||$ [20]. It should be emphasised that the unit vector $\mathbf{t} = -\boldsymbol{\delta}_{el}/||\boldsymbol{\delta}_{el}||$ is calculated taking the vector $\boldsymbol{\delta}_{el}$ given by Eq. (39) i.e. before recalculation of the $\boldsymbol{\delta}_{el}$ by Eqs. (35) and (37). For more clarity see Fig. 3.

It is evident, that the unit vector $-\mathbf{v}_{C,t}/||\mathbf{v}_{C,t}||$ are not parallel neither to $\mathbf{F}_{t,st}/||\mathbf{F}_{t,st}||$ nor to $-\boldsymbol{\delta}_{el}/||\boldsymbol{\delta}_{el}||$. However, it is not clear apparently that the other two vectors i.e. $-\boldsymbol{\delta}_{el}/||\boldsymbol{\delta}_{el}||$ and $\mathbf{F}_{t,st}/||\mathbf{F}_{t,st}||$ are not parallel to each other. Let us show it. Let us show at the beginning, that the increment of the static frictional force $\Delta\mathbf{F}_{t,st}(t_m)$ and increment of the tangential elastic displacement $\Delta\boldsymbol{\delta}_{el}(t_m)$ are opposite parallel (antiparallel) vectors to each other. Here $\Delta\mathbf{F}_{t,st}(t_m)$ is defined in (28) and $\Delta\boldsymbol{\delta}_{el}(t_m)$ is defined in (39) together with (38). Taking into account the property of the generalized mean (40) of the integral (28), the increment $\Delta\mathbf{F}_{t,st}(t_m)$ may be represented as follows

$$\Delta\mathbf{F}_{t,st}\left(t_m\right) = k_t\left(\xi\right)\int\limits_{t_{m-1}}^{t_m}\frac{d\boldsymbol{\delta}_{el}(\tau)}{d\tau}d\tau. \tag{49}$$

At the beginning of the calculation of the $\mathbf{F}_t$ in every cycle (see Fig. 3) we assume that the Coulomb limit is not reached i.e. $||\mathbf{F}_{t,st}(t)|| < \mu||\mathbf{F}_n(t)||$ as $t \in [t_{m-1}, t_m]$, then the increment of the elastic displacement $\boldsymbol{\delta}_{el}(t)$ coincides with the increment of the total displacement $\mathbf{s}(t)$. Therefore, the time derivative of the elastic displacement $d\boldsymbol{\delta}_{el}(t)/dt$ is the relative velocity of the contact point $\mathbf{v}_{C,t}(t)$. Therefore, the integral of Eq. (49) is equal to the increment $\Delta\boldsymbol{\delta}_{el}(t_m)$ according to (39) and (38). Consequently, we have $\Delta\mathbf{F}_{t,st}(t_m) = -k_t(\xi)\Delta\boldsymbol{\delta}_{el}(t_m)$. It is evident that the vectors $\Delta\boldsymbol{\delta}_{el}(t_m)$ and $-k_t(\xi)\Delta\boldsymbol{\delta}_{el}(t_m)$ are antiparallel. If we assume that $\mathbf{F}_{t,st}(t_{m-1})$ is parallel to $\boldsymbol{\delta}_{el}(t_{m-1})$, then the vectors $\mathbf{F}_{t,st}(t_m) = \mathbf{F}_t(t_{m-1}) - k_t(\xi)\Delta\boldsymbol{\delta}_{el}(t_m)$ and $\boldsymbol{\delta}_{el}(t_m) = \boldsymbol{\delta}_{el}(t_{m-1}) + \Delta\boldsymbol{\delta}_{el}(t_m)$ cannot be parallel due to parallelism of the $\Delta\boldsymbol{\delta}_{el}(t_m)$ and $-k_t(\xi)\Delta\boldsymbol{\delta}_{el}(t_m)$. It is illustrated clearly in Fig. 7. Since $\mathbf{F}_{t,sl}(t_m)$ and $\boldsymbol{\delta}_{el}(t_m)$ are not parallel, then $\mathbf{F}_{t,st}/||\mathbf{F}_{t,st}||$ and $-\boldsymbol{\delta}_{el}/||\boldsymbol{\delta}_{el}||$ are not equal or parallel, either. In one-dimensional case the vectors $\mathbf{F}_{t,st}/||\mathbf{F}_{t,st}||$ and $-\boldsymbol{\delta}_{el}/||\boldsymbol{\delta}_{el}||$ may be equidirectional or antiparallel.

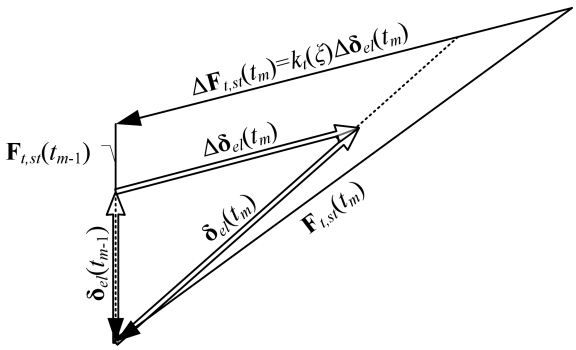

Fig. 7. The scheme for proving that the vectors $\mathbf{F}_{t,st}(t_m)$ and $\boldsymbol{\delta}_{el}(t_m)$ are not parallel

However, if tangential stiffness k_t is constant during the contact, then it is evident that $\mathbf{F}_{t,st}(t_m)$ given by (21) and $\boldsymbol{\delta}_{el}(t_m)$ given by (39) are parallel vectors, since $\mathbf{F}_{t,st}(t_m)$ differs from $-\boldsymbol{\delta}_{el}(t_m)$ only in the factor k_t.

Let us, at the beginning, consider differences between vectors $-\mathbf{v}_{C,t}/||\mathbf{v}_{C,t}||$ and $\mathbf{F}_{t,st}/||\mathbf{F}_{t,st}||$ or $-\mathbf{v}_{C,t}/||\mathbf{v}_{C,t}||$ and $-\boldsymbol{\delta}_{el}/||\boldsymbol{\delta}_{el}||$ by employing simple one-dimensional oscillator without damping. This model is suitable to illustrate one dimensional tangential behaviour of a single particle on a plane in neighborhood of the point at which pure rolling condition $\mathbf{v}_{C,t} = 0$ is realized when the normal force $\mathbf{F}_n = \textit{constant}$ during the contact, and only two forces, $\mathbf{F}_{t,st}$ and the inertial force, affect particle. In this case the tangential motion of the contact point of the particle can be described as follows [15, 30]

$$m\frac{d^2\delta_{el}\left(t\right)}{dt^2} + k_t\delta_{el}\left(t\right)r = 0, \tag{50}$$

where $\delta_{el} = x + R\vartheta$ can be assumed as the displacement of the contact point, $r = 1 + (mR^2/I) = 7/2$ is the non-dimensional radius, m, R and I are the mass, radius and moment of inertia of the particle, respectively, θ is the angular displacement, k_t is the tangential stiffness and x is the displacement of the mass centre of the particle. If the initial relative velocity of the contact point equals zero, then the solution of Eq. (50) is as follows

$$\delta_{el}(t) = \delta_{el}(t_0)\cos\left(t\sqrt{k_t/m}\right), \tag{51}$$

where $\delta_{el}(t_0)$ is the initial displacement. Since the stiffness $k_t = const$ during the contact, then, in this case, $F_{t,st}(t) = k_t\delta_{el}(t)$. The relative tangential velocity of the contact point is defined as the time derivative of (51). Explicitly,

$$v_{C,t}(t) = -\sqrt{k_t/m}\,\delta_{el}(t_0)\sin\left(t\sqrt{k_t/m}\right). \tag{52}$$

In order to calculate the displacement and velocity of the contact point according to Eqs. (51) and (52) the same particle was considered as in the previous 4th section. The remaining parameters of Eqs. (50) and (52) are the following: $k_t = 1.905 \cdot 10^5$ N/m and $\delta_{el}(t_0) = mg\mu/k_t = -0.808 \cdot 10^{-5}$ m. The contact point displacement $\delta_{el}(t)$, relative velocity $v_{C,t}(t)$, tangential force $F_{t,st}(t)$ and their ratios $F_{t,st}/||F_{t,st}||$, $-\delta_{el}/||\delta_{el}||$ and $-v_{C,t}/||v_{C,t}||$, for the considered particle, are depicted in Fig. 8.

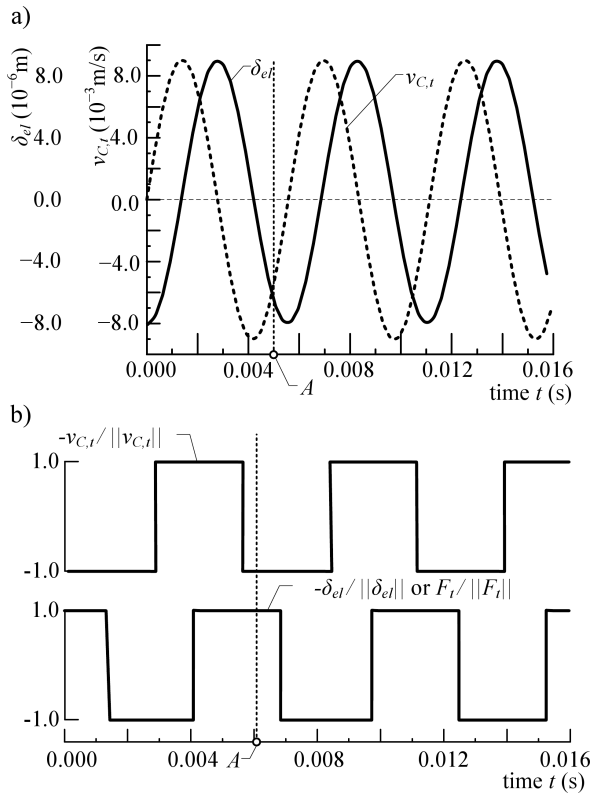

Fig. 8. Motion parameters of the contact point according to Eqs. (51) and (52): a) relative displacement δ_{el} and relative speed $v_{C,t}$, b) ratios $F_{t,st}/||F_{t,st}||$, $-\delta_{el}/||\delta_{el}||$, and $-v_{C,t}/||v_{C,t}||$

As we can see from Fig. 8b, the ratios $F_{t,st}/||F_{t,st}||$ and $-\delta_{el}/||\delta_{el}||$ differ from $-v_{C,t}/||v_{C,t}||$. More precisely, their directions are opposite during certain time intervals. The differences between $F_{t,st}/||F_{t,st}||$ and $-v_{C,t}/||v_{C,t}||$ or between $-\delta_{el}/||\delta_{el}||$ and $-v_{C,t}/||v_{C,t}||$ are demonstrated in one dimensional case; however, in 2D case these differences should remain the same. As a consequence, if the unit vector is $-v_{C,t}/||v_{C,t}||$ and at the point A the Coulomb limit becomes reached the behaviour of $F_{t,st}$ is unrealistic and inconsistent with physics and other versions of the unit vectors (Fig. 9c).

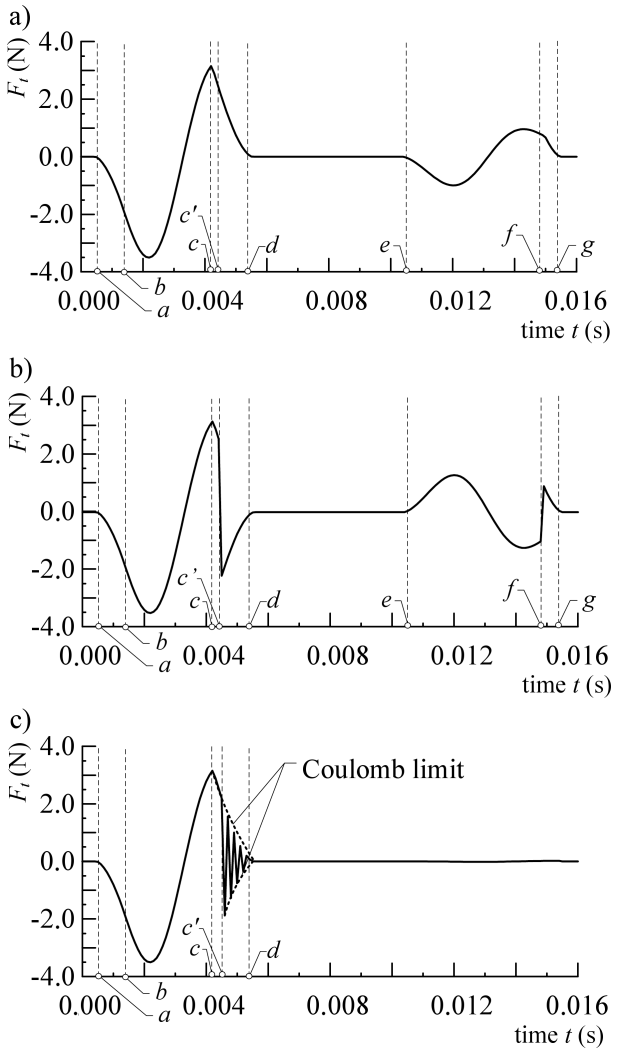

Fig. 9. The dependences of tangential force on direction vector $\mathbf{t}$ of Eq. (19): a) when $\mathbf{t} = \mathbf{F}_{t,st}/||\mathbf{F}_{t,st}||$, b) when $\mathbf{t} = -\boldsymbol{\delta}_{el}/||\boldsymbol{\delta}_{el}||$ and c) when $\mathbf{t} = -\mathbf{v}_{C,t}/||\mathbf{v}_{C,t}||$

Our further investigation is addressed to a detailed analysis of three unit vectors $\mathbf{t}$ by applying theoretical and numerical methods.

We shall consider three unit vectors $\mathbf{t}$ of Eq. (19): $\mathbf{t} = -\mathbf{v}_{C,t}/||\mathbf{v}_{C,t}||$, $\mathbf{t} = \mathbf{F}_{t,st}/||\mathbf{F}_{t,st}||$ and $\mathbf{t} = -\delta_{el}/||\delta_{el}||$, in the one dimensional case of the particle, which was discussed earlier. It is found out that the behaviour of tangential force is usually evaluated properly with all the three versions of the vector $\mathbf{t}$ when so-called pure rolling condition $v_{C,t} = 0$, while the Coulomb limit is reached, is not realized. However, the behaviour of the frictional force is different when the

Coulomb limit is reached, i.e. $||\mathbf{F}_{t,st}|| > \mu||\mathbf{F}_n||$, and condition $\mathbf{v}_{C,t} = 0$ is realised at the certain time of the contact.

In Fig. 9 the segments between points a and d mean the same interaction modes as in Fig. 5. The point e in Fig. 9 denotes beginning of the second contact of the particle. The segment e–f corresponds to the stick mode while the segment f–g corresponds to the sliding mode. The time when the relative velocity of the contact point $\mathbf{v}_{C,t} = 0$ is realized is denoted by the point c'.

If we take in (19) that $\mathbf{t} = -\boldsymbol{\delta}_{el}/||\boldsymbol{\delta}_{el}||$, then nonphysical jump occurs under considered conditions in tangential force diagram (see Fig. 9b) at the moment when $\mathbf{v}_{C,t} = 0$ (c' point). It happens so because the directions of the vector $\boldsymbol{\delta}_{el}(t)$ in the neighbourhood of the point c', i.e. when $t < t_{c'}$ and $t \geq t_{c'}$, are opposite (Fig. 9b); however, $\mathbf{F}_{t,st}$ keeps the same sign in the neighbourhood of the point c'. It can seem strange, because $\mathbf{F}_{t,st} \neq 0$ as $\boldsymbol{\delta}_{el} = 0$ and $\mathbf{F}_{t,st}$ does not change its sign as $\boldsymbol{\delta}_{el}$ does it. However, it happens due to alternating $\mathbf{F}_n$ with respect to time, which causes alternation of k_t, and in this case, the incremental approaches (27), (28) and (29) lead to $\mathbf{F}_{t,st} \neq 0$ as $\boldsymbol{\delta}_{el} = 0$. In addition, due to alternating k_t, the tangential force $\mathbf{F}_{t,st}$ keeps the same sign in the neighbourhood of the point c' while the direction of $\boldsymbol{\delta}_{el}$ is different in the same neighbourhood. We would like to remind again that $\mathbf{t} = -\boldsymbol{\delta}_{el}/||\boldsymbol{\delta}_{el}||$ is calculated by taking $\boldsymbol{\delta}_{el}$ according to the formula (39) i.e. before recalculation of the $\boldsymbol{\delta}_{el}$ by (35) and (37). In Fig. 5b depicted $\boldsymbol{\delta}_{el}$ is calculated by Eqs. (35) and (37) when the Coulomb limit is reached, and it does not reflect exactly $\boldsymbol{\delta}_{el}$ calculated by (39).

If we take the velocity approach $\mathbf{t} = -\mathbf{v}_{C,t}/||\mathbf{v}_{C,t}||$ in (19), then nonphysical oscillations of the tangential force $\mathbf{F}_t$ occur with each step from the moment when $\mathbf{v}_{C,t} = 0$ (c' point) till the end of the contact (Fig. 9c). This phenomenon can be explained by the fact that the average value of the force $\mathbf{F}_t$ as $t \geq t_{c'}$ equals zero, here $t_{c'}$ is the time instant at the point c'. It can be understood from Fig. 9c, why oscillations are symmetric with respect to zero value of $\mathbf{F}_t$. Since the average value of the $\mathbf{F}_t$ is zero, then average value of the velocity of the tangential component of the contact point does not change from point c' till the end of the contact. Since $\mathbf{v}_{C,t} = 0$ at the point c' and it does not change from that time up to end of the contact, then $\mathbf{v}_{C,t} = 0$ at the end of the first contact, and during the second contact as well. However, in other cases of the unit vector $\mathbf{t}$, the frictional force does not equal zero. No jump or oscillations occur in $\mathbf{F}_t$ graph if we take that $\mathbf{t} = \mathbf{F}_{t,st}/||\mathbf{F}_{t,st}||$ (see Fig. 9a). Variation of tangential force seems to be physically correct with monotonic switch at transition points.

It should be emphasised that there is a contradiction in the use of the unit vectors $-\mathbf{v}_{C,t}/||\mathbf{v}_{C,t}||$, $\mathbf{F}_{t,st}/||\mathbf{F}_{t,st}||$ and $-\boldsymbol{\delta}_{el}/||\boldsymbol{\delta}_{el}||$ in the discrete element method and in modelling of the rigid body dynamics in general. The commonly accepted Coulomb's dry friction law is as follows $\mathbf{F}_t = -\mu\mathbf{F}_n(\mathbf{v}_{C,t}/||\mathbf{v}_{C,t}||)$ as $\mathbf{v}_{C,t} \neq 0$, see for example [26]. As a rule, other unit vectors, i.e. $\mathbf{F}_{t,st}/||\mathbf{F}_{t,st}||$ and $-\boldsymbol{\delta}_{el}/||\boldsymbol{\delta}_{el}||$, if $\mathbf{v}_{C,t} \neq 0$ are not used in modelling of the rigid body dynamics. The problem arises when velocity at the contact point $\mathbf{v}_{C,t} = 0$. In this case, according to Coulomb's dry friction law, the direction of the $\mathbf{F}_t$ and its magnitude are not defined; it is only known that $\mathbf{F}_t < \mu||\mathbf{F}_n||$. To avoid these uncertainties Coulomb's law is regularized. The regularization may be implemented with respect to the tangential velocity $\mathbf{v}_{C,t}$ [26], or with respect to the elastic tangential displacement $\boldsymbol{\delta}_{el}$, as it was done in the present article. It should be noted that the regularisation modified magnitude of the tangential force $\mathbf{F}_t$ but not its direction. Therefore, in general, it is evident that the directions of the $\mathbf{F}_t$ are different when regularisation is implemented with respect to the velocity $\mathbf{v}_{C,t}$ or with respect to the elastic displacement $\boldsymbol{\delta}_{el}$ or stick force $\mathbf{F}_{t,st}$. Regarding to previous reasoning, in three dimensional modelling, the direction vector should be $-\mathbf{v}_{C,t}/||\mathbf{v}_{C,t}||$ as $\mathbf{v}_{C,t} \neq 0$. However, as it is shown above even in the sliding mode, when the Coulomb limit is reached, the behaviour of $\mathbf{F}_t$ is not correct if $\mathbf{t} = -\mathbf{v}_{C,t}/||\mathbf{v}_{C,t}||$, because nonphysical oscillations occur, see Fig. 9c on the right of the point c'. The performed analysis showed that problem of the direction of the frictional force still remains unresolved fully.

6. Conclusions

It was found out that the existing methodology under variable normal loading causes the non-physical discontinuity of the elastic and sliding components of the tangential displacement of the contact point at the stick–sliding transition point when the Coulomb limit is reached. The suggested incrementally linear, history dependent methodology does not have mentioned disadvantage. The suggested methodology allows us to calculate the elastic and sliding component of the tangential displacement of the contact point more precisely than the existing methodology. It was shown that the existing methodology is suitable only when the stiffness of the tangential interaction is constant during the contact, or in other words, when normal loading is constant during the contact.

The unit vector based on the stick tangential force showed the most reliable results among investigated three versions of the unit vectors. This vector leads to smooth behaviour of the tangential force without non-physical oscillations. The unit vector based on the elastic displacement of the contact point showed worse results. This vector may lead to non-physical jump of the tangential force. The unit vector based on the relative tangential velocity of the contact point may lead to non-physical oscillations of the tangential force within the time interval from the time when pure rolling condition is realized and till the end of the contact. The unrealistic behaviour of the tangential force artificially affects dynamics of the particle as well. The results of the numerical experiments showed a contradiction between the conventional unit vector based on the tangential velocity and the other two considered unit vectors. The conducted analysis showed that the issue of the unit vectors needs more detailed investigation.

Appendix. The method of the integration

The equations of the motion (2) and (3) given in the form of coupled ordinary differential equations need to be solved

over the time. By applying the incremental approach, these equations can be solved numerically by explicit, implicit or predictor-corrector schemes and the new positions and velocities for the upcoming time step are available. The explicit numerical integration schemes considering the discrete element method are reviewed by Džiugys and Peters [4] and Kruggel-Emden [31]. Performance of numerical integrators on tangential motion of DEM within implicit flow solvers is presented by Jasion [32].

Various integrations methods can be used to integrate differential equations (2) and (3): Verlet, Gear's predictor-corrector, Newmark predictor-corrector, Adams-Bashforth multistep, and Adams-Moulton predictor-corrector [23, 24, 32–35]. The algorithmic diagram illustrating the predictor-corrector loop in time increment $t + \Delta t$ is shown in Fig. 10.

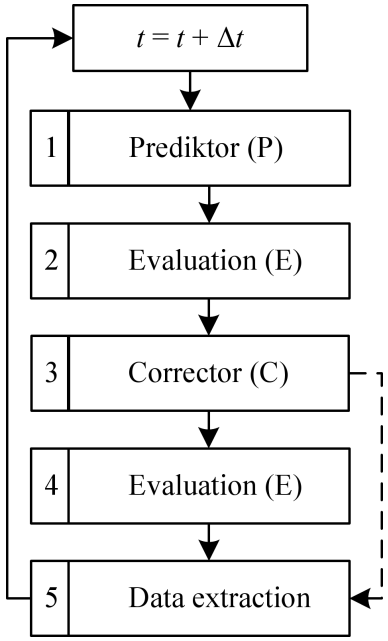

Fig. 10. A general DEM scheme using the predictor-corrector method

In the predictor stage, denoted by P, the approximate values of the positions $\mathbf{x}^p$, rotations $\boldsymbol{\theta}^p$, linear $\mathbf{v}^p$ and angular $\boldsymbol{\omega}^p$ velocities and, if necessary, their higher-order derivatives are evaluated. The evaluation stage, denoted by E, involves calculation of the interaction parameters by using the predicted values of the position and velocity. The correction stage, denoted by C, involves the calculation of the corrected values of the positions and velocities in Eqs. (2) and (3), by using interaction parameters that are calculated in 2^{nd} item. Item 4 indicates the recalculation of interaction parameters using corrected values of the positions and velocities. The last item of the incremental loop is required for the final arrangement, calculation and recording of necessary data.

There are many possibilities for realization of the predictor-corrector method (Butcher J.C. (2008) [36]): *PEC*, *PECE*, *PECEC* or in general $P(EC)^k$ or $P(EC)^kE$. The evaluation of the interaction forces requires the biggest part of the computational time. Therefore, in the DEM, the *PEC* scheme is mostly used [23, 34]. The *PECEC* scheme is rarely used [24]. The 2^{nd} and 4^{th} steps of the integration scheme (Fig. 10) were explained in the block scheme of the calculation of the interaction parameters (Fig. 3).

Taking into account criticism of the Gear predictor-corrector method [37], in the present investigation, the Newmark predictor-corrector method is implemented within the simplest *PEC* scheme as shown in Fig. 10.

Velocities and positions at time instant t_m in the predictor step are calculated as follows:

$$\mathbf{v}^p(t_m) = \mathbf{v}(t_{m-1}) + 0.25\Delta t\mathbf{F}(t_{m-1})/m, \tag{53}$$

$$\mathbf{x}^p(t_m) = \mathbf{x}(t_{m-1}) + \Delta t\mathbf{v}(t_{m-1}) + 0.25\Delta t^2\mathbf{F}(t_{m-1})/m, \tag{54}$$

$$\boldsymbol{\omega}^p(t_m) = \boldsymbol{\omega}(t_{m-1}) + 0.25\Delta t\mathbf{M}(t_{m-1})/I, \tag{55}$$

$$\boldsymbol{\theta}^p(t_m) = \boldsymbol{\theta}^p(t_{m-1}) + \Delta t\boldsymbol{\omega}(t_{m-1}) + 0.25\Delta t^2\mathbf{M}(t_{m-1})/I. \tag{56}$$

In the corrector step, they are:

$$\mathbf{v}^c(t_m) = \mathbf{v}^p(t_m) + 0.5\Delta t\mathbf{F}^p(t_m)/m, \tag{57}$$

$$\mathbf{x}^c(t_m) = \mathbf{x}^p(t_m) + 0.25\Delta t^2\mathbf{F}^p(t_m)/m, \tag{58}$$

$$\boldsymbol{\omega}^c(t_m) = \boldsymbol{\omega}^p(t_m) + 0.5\Delta t\mathbf{M}^p(t_{m-1})/I, \tag{59}$$

$$\boldsymbol{\theta}^c(t_m) = \boldsymbol{\theta}^p(t_m) + 0.25\Delta t^2\mathbf{M}^p(t_m)/I. \tag{60}$$

REFERENCES

[1] P.A. Cundall and O.D.L. Strack, "A discrete numerical model for granular assemblies", *Geotechnique* 29, 47–65 (1979).

[2] R.D. Mindlin, "Compliance of elastic bodies in contact", *J. Appl. Mechanics* 16, 259–268 (1949).

[3] R.D. Mindlin and H. Deresiewicz, "Elastic spheres in contact under varying oblique forces", *J. Appl. Mechanics* 20, 327–344 (1953).

[4] A. Džiugys and B.J. Peters, "An approach to simulate the motion of spherical and non-spherical fuel particles in combustion chambers", *Granular Material* 3, 231–266 (2001).

[5] Y. Zhou, R.Y. Yang, and A.B. Yu, "Discrete particle simulation of particulate systems: theoretical developments", *Chemical Eng. Science* 62, 3378–3392 (2007).

[6] H. Kruggel-Emden, S. Wirtz, and V. Scherer, "Applicable contact force models for the discrete element method: the single particle perspective", *J Pressure Vessel Technology* 131, 2024001–2024011 (2009).

[7] C. Thornton, S.J. Cummins, and P.W. Cleary, "An investigation of the comparative behaviour of alternative contact force models during elastic collisions", *Powder Technology* 210 (3), 189–197 (2011).

[8] X. Zhang and L. Vu-Quoc, "An accurate elasto-plastic frictional tangential force-displacement model for granular-flow simulations: displacement-driven formulation", *J Computational Physics* 225 (1), 730–752 (2007).

[9] L. Vu-Quoc and X. Zhang, "An accurate and efficient tangential force-displacement model for elastic frictional contact in particle-flow simulations", *Mechanics of Materials* 31, 235–269 (1999).

[10] H. Kruggel-Emden, S. Wirtz, and V. Scherer, "A study on tangential force laws applicable to the discrete element method (DEM) for materials with viscoelastic or plastic behaviour", *Chemical Eng. Sci.* 63, 1523–1541 (2008).

[11] H. Kruggel-Emden, E. Simsek, S. Rickelt, S. Wirtz, and V. Scherer, "Review and extension of normal force models for the discrete element method", *Powder Technology* 171, 157–173 (2006).

[12] O.R. Walton and R.L. Braun, "Viscosity, granular temperature and stress calculations for shearing assemblies of inelastic, frictional disks", *J Rheology* 30, 949–980 (1986).

[13] Y. Tsuji, T. Tanaka, and T. Ishida, "Lagrangian numerical simulation of plug flow of cohesionless particles in a horizontal pipe", *Powder Technology* 71, 239–250 (1992).

[14] A. Di Renzo and F.P. Di Maio, "Comparison of contact-force models for the simulation of collisions in DEM-based granular flow codes", *Chemical Eng. Sci.* 59, 525–541 (2004).

[15] F.P. Di Maio and A. Di Renzo, "Analytical solution for the problem of frictional-elastic collisions of spherical particles using the linear model", *Chemical Eng. Sci.* 59 (16), 3461–3475 (2004).

[16] N.V. Brilliantov, F. Spahn, J. Hertzsch, and T. Poeschel, "Model for collisions in granular gases", *Physical Review* E 53 (5), 5382–5392 (1996).

[17] P. Van Liedekerke, E. Tijskens, E. Dintwa, J. Anthonis, and H. Ramon, "A discrete element model for simulation of a spinning disc fertilizer spreader I. Single particle simulations", *Powder Technology* 170, 71–85 (2006).

[18] H.P. Zhu and A.B. Yu, "The effects of wall and rolling resistance on the couple stress of granular materials in vertical flow", *Physica* A 325, 347–360 (2003).

[19] P.K. Haff and R.S. Anderson, "Grain scale simulations of loose sedimentary beds: the example of grain-bed impacts in aeolian saltation", *Sedimentology* 40, 175–198 (1993).

[20] E. Oñate and J. Rojek, "Combination of discrete element and finite element methods for dynamic analysis of geomechanics problems", *Comput. Meth. Appl. Mech. Eng.* 193, 3087–3128 (2004).

[21] S. Luding, "Shear flow modelling of cohesive and frictional fine powder", *Powder Technology* 158, 45–501 (2005).

[22] J. Argyris, "An excursion into large rotations", *Comput. Meth. Appl. Mech. Eng.* 32, 85–155 (1982).

[23] T. Poschel and T. Schwager, *Computational Granular Dynamics: Models and Algorithms*, Springer, Berlin, 2010.

[24] M.P. Allen and D.J. Tildesley, *Computer Simulation of Liquids,* Clarendon Press, London, 2008.

[25] R. Michalowski and Z. Mróz, "Associated and non-associated sliding rules in contact friction problems", *Archives of Mechanics* 30 (3), 259–276 (1978), (in Polish).

[26] P. Wriggers, *Computational Contact Mechanics*, Wiley, London, 2002.

[27] G.A. Kohring, "Studies of diffusional mixing in rotating drums via computer simulations", *J. Phys. I France* 5, 1551–1561 (1995).

[28] J.S. Leszczynski, "A discrete model of a two-particle contact applied to cohesive granular materials", *Granular Matter* 5 (2), 91–98 (2003).

[29] D. Zhang and W.J. Whiten, "A new calculation method for particle motion in tangential direction in discrete element simulations", *Powder Technology* 102 (3), 235–243 (1999).

[30] H. Kruggel-Emden, S. Wirtz, and V. Scherer, "An analytical solution of different configuration of the linear viscoelastic normal and frictional-elastic tangential contact model", *Chemical Eng. Sci.* 62, 6914–6926 (2007).

[31] H. Kruggel-Emden, M. Sturm, S. Wirtz, and V. Scherer, "Selection of an appropriate time integration scheme for the discrete element method (DEM)", *Computers & Chemical Eng.* 32 (10), 2263–2279 (2008).

[32] G. Jasion, J. Shrimptona, M. Danbya, and K. Takedab. "Performance of numerical integrators on tangential motion of DEM within implicit flow solvers", *Computers & Chemical Eng* 35 (11), 2218–2226 (2011).

[33] D. Frenkel and B. Smit, *Understanding Molecular Simulation from Algorithm to Applications*, Academic Press, New York, 2001.

[34] J.M. Haile, *Molecular Dynamics Simulation: Elementary Methods*, Wiley-Interscience, London, 1992.

[35] P. Deuflhard, J. Hermans, B. Leimkuhler, A.E. Mark, S. Reich, and R.D. Skeel, "Computational molecular dynamics: challenges, methods, ideas", 2^{nd} *Proc. Int. Symposium on Algorithms for Macromolecular Modelling* 1, CD-ROM (1998).

[36] J.C. Butcher, *Numerical Methods for Ordinary Differential Equations*, John Wiley & Sons Ltd, London, 2008.

[37] B.J. Min, "Anomalous behavior of gear's predictor-corrector algorithm in a molecular dynamics simulation of amorphous silicon", *J. Korean Physical Society* 57 (5), 1153–1157 (2010).